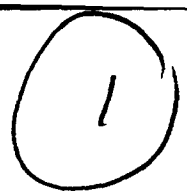

Final Report for Period June 1981 to September 1981

FORMULATION OF THE ANALYSIS FOR NONLINEAR AEROSOL THERMAL BLOOMING

Prepared by

James Wallace
Far Field, Inc.
6 Thoreau Way, Sudbury, Massachusetts 01776

October 1981

Prepared for

U.S. Army Missile Command
Redstone Arsenal, Alabama 35898

Under

Contract DAAH01-81-C-A810

DISCLAIMER NOTICE

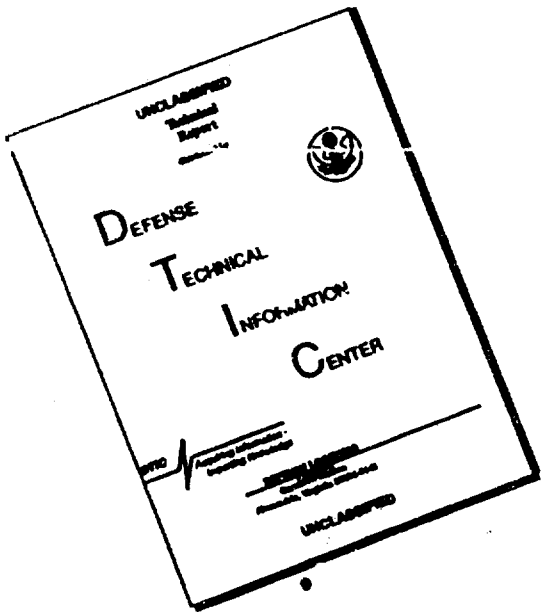

THIS DOCUMENT IS BEST QUALITY AVAILABLE. THE COPY FURNISHED TO DTIC CONTAINED A SIGNIFICANT NUMBER OF PAGES WHICH DO NOT REPRODUCE LEGIBLY.

ACKNOWLEDGEMENT

This report was prepared by Far Field, Inc., 6 Thoreau Way, Sudbury, Massachusetts, 01776, under Contract DAAH01-81-C-A810 with the U.S. Army Missile Command.

The views and conclusions contained in this report are those of the author and should not be interpreted as representing the official policies, either expressed or implied, of the U.S. Army Missile Command or the U.S. Government.

Effective Date of Contract:	May 20 ,1981
Contract Expiration Date:	September 30, 1981
Amount of Contract:	$35,000
Principal Investigator:	Dr. James Wallace

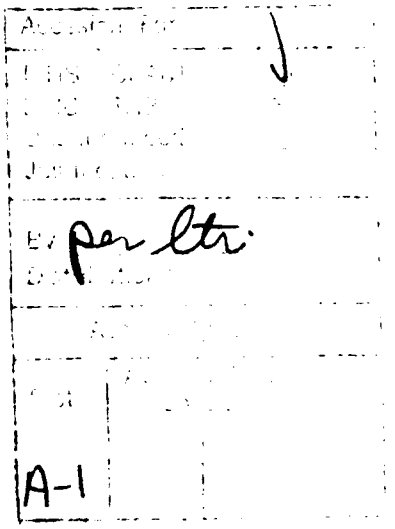

Formulation of the Analysis for Nonlinear Aerosol Thermal Blooming

James Wallace

Far Field, Inc., Sudbury, Massachusetts 01776

In this paper we present a theoretical analysis for the interaction of a high-energy laser beam with a hygroscopic aerosol. Droplet absorption simultaneously heats the atmosphere and vaporizes the droplet. When a droplet is vaporized a thin, non-equilibrium region exists at the droplet surface. This interfacial discontinuity determines the amount of droplet superheat as a function of the rate of vaporization. For submicron droplets the degree of superheat achieved is small because heat conduction to the atmosphere keeps the droplets cool. Less than ten percent of the absorbed energy is available for vaporization. Droplets larger than 1μm are heated to higher temperatures with as much as ninety percent of the absorbed energy available for vaporization. After the large droplets are vaporized to submicron size the residual droplets scatter, absorb and thermally bloom the laser beam as if they are non-vaporizing.

I. INTRODUCTION

There have been several theoretical and experimental investigations[1-12] on the interaction of a high-energy laser beam with hygroscopic aerosols. This problem is of interest because the absorbed energy can vaporize the droplets and increase the meteorlogical range. However energy transport between the heated droplet and the atmosphere simultaneously occurs with vaporization and reduces the energy available for vaporization. In this paper we present the analysis for determining the fraction of absorbed energy that results in vaporization. The remainder of the absorbed energy is deposited into the atmosphere as heat and causes thermal blooming. To accomplish this we require a rather detailed treatment of both the thermodynamics and hydrodynamics of a vaporizing droplet.

When a droplet is vaporized a very thin but finite non-equilibrium region exists at the droplet surface to allow for the phase transaction. This interfacial discontinuity requires a saturated vapor pressure at the droplet temperature that is higher than the actual vapor pressure at the droplet surface. The droplet is said to be superheated with the degree of superheat dependent upon the rate of vaporization. The non-equilibrium theory requires high droplet temperatures and increases the energy deposited into the atmosphere as heat. Energy transport from the droplet to the atmosphere occurs either gas dynamically or by diffusion. Convective or gas dynamic vaporization occurs whenever the vapor pressure at the droplet surface is greater than the ambient pressure. As evaporation proceeds the droplet becomes smaller and the absorbed irradiance, droplet temperature, and vapor pressure all decrease. When the vapor pressure at the droplet surface becomes less than the ambient pressure diffusion determines the rate of energy transport into the atmosphere. For submicron

droplets the degree of superheat required for rapid vaporization cannot be achieved because heat conduction into the atmosphere keeps the droplets cool. Vaporization of submicron droplets is said to be kinetically limited with less than ten percent of the absorbed energy available for vaporization. Vaporization of large droplets is not kinetically limited and up to ninety percent of the absorbed energy is available for vaporization. Thus, an order of magnitude larger irradiance is required to evaporate a submicron droplet at the same relative rate as a 10μm droplet. Even if the energy for complete vaporization is available the non-equilibrium theory of evaporation imposes a limit on the final droplet size that can be attained. A high-energy laser beam propagates through the resulting haze as if the droplets are non-vaporizing. The residual droplets scatter, absorb and thermally bloom the laser beam.

Because the droplets are superheated they can be shattered rather than vaporized. The same nucleation phenomena that occurs in boiling and cavitating flows can also occur in heated droplets. Nucleation[13] is the formation of vapor cavities in the interior of the droplet. The droplet will be shattered when the saturated vapor pressure at the droplet temperature exceeds the limiting tensile stress of the droplet. The temperature at which vapor cavities are formed is called the incipient boiling temperature. At one atmosphere this temperature varies from a few degrees in excess of 100°C when entrapped air is present to 267°C in pure water[13].

II. VAPORIZATION MODEL

The interaction of a laser beam with aerosol droplets that are vaporized is complicated by non-equilibrium thermodynamics[14]. When two phases exist in equilibrium the second law requires continuity of temperature and the free energy. However with a finite rate of mass transport the two phases are no longer in equilibrium and a thin transition layer is required. Experimental evidence indicates that the thickness of the layer is a few mean free paths(10^{-6} cm) and is accompanied by steep gradients in the vapor pressure. The net mass flux across the interface is the difference between the Langmuir rate of evaporation of a pure liquid into a vacuum and the rate of condensation of vapor molecules on a liquid surface and has been given by Schrage[15] as

$$\dot{m} = \epsilon(p^s(T_p) - F(v)p)/(2\pi R_v T_p)^{\frac{1}{2}}, \qquad (1)$$

where ϵ is the evaporation(= condensation) coefficient, p^s is the saturated vapor pressure of the droplet, p is the actual vapor pressure of the droplet, T_p is the temperature of the droplet and $R_v = 0.462 J/gm\text{-}^{o}K$ is the gas constant for water vapor. The function $F(v)$ represents the influence of the bulk velocity moving away from the droplet and is given by

$$F(v) = \exp(-v^2/2R_v T_p) - (\pi/2R_v T_p)^{\frac{1}{2}} v(1 - \mathrm{erf}(v/(2R_v T_p)^{\frac{1}{2}})); \quad v = \dot{m}/\rho. \qquad (2)$$

A small temperature jump[16] also occurs across the liquid-vapor interface but it has been neglected. The physical explanation of Eq. (1) follows from the kinetic

theory of gases. As the droplet evaporates the vapor molecules collide with other molecules and attain a random velocity distribution. Some of the vapor molecules also collide with the droplet and reattach. The fraction of vapor molecules that stick to the droplet is the condensation(=evaporation) coefficient with the remaining vapor molecules reflected from the droplet. The published values of the evaporation coefficient vary from 1.0 in a vacuum to 0.04 at one atmosphere[16]. When the bulk velocity equals or exceeds the mean thermal speed $(2R_vT_p)^{\frac{1}{2}}$ F is small because few vapor molecules have a velocity in the direction opposite to the bulk velocity that is large enough to cause a collision and subsequent reattachment to the droplet.

Net evaporation occurs when the saturated vapor pressure $p^s(T_p)$ of the droplet exceeds the actual vapor pressure in the gas. Net condensation occurs when the saturated vapor pressure of the droplet is less than actual vapor pressure. The non-equilibrium theory requires superheating of the vapor for evaporation and subcooling of the vapor for condensation. After replacing ρ by p/R_vT_p in $\dot{m}$ we can determine,from Eq.(1), the ratio of the saturated vapor pressure $p^s(T_p)$ to the actual vapor pressure p as a function of the Mach number $v/(\gamma R_vT_p)^{\frac{1}{2}}$ of the vapor. This is shown in Fig.1. For an evaporation coefficient of 1 significant non-equilibrium effects occur for Mach numbers greater than 0.5. For an evaporation coefficient of 0.04 non-equilibrium effects are dominant for virtually all Mach numbers. Also shown in Fig.1 are the asymptotes where recondensation is negligible and the vacuum rate of evaporation applies.

Under the assumption that the temperature is uniform across the droplet

mass conservation and an energy balance at the droplet surface gives the following relationships between the droplet radius, temperature and rate of evaporation;

$$\rho_p \dot{\sigma} = -\dot{m} \; ; \quad \dot{m}\,(L + h_v(T_p) - h_v(T_\infty) + v^2/2) + \kappa T_r + \sigma \rho_p C T_t/3 = IQ_a/4 \; , \qquad (3)$$

where σ is the droplet radius, $\rho_p = 1\ \mathrm{gm/cm^3}$ is the density of the droplet, $\dot{m}$ is the rate of vaporization, $C = 4.2\ \mathrm{J/gm\text{-}^oK}$ is the specific heat of water, T_p is the droplet temperature, $L = 2500\ \mathrm{J/gm}$ is the latent heat, h_v is the enthalpy of the vapor, v^2 is the convective velocity of the vapor, $\kappa = 2.55 \times 10^{-4}\ \mathrm{J/cm\text{-}sec\text{-}^oK}$ is the thermal conductivity of air, I is the irradiance and Q_a is the Mie absorption coefficient of the droplet. When the latent heat dominates the other terms in Eq. (3) most of the absorbed irradiance will result in droplet vaporization. To determine when this occurs we must first solve the conservation equations in the atmosphere for the vapor pressure p and temperature gradient T_r. This is discussed in the next section.

III. MASS AND ENERGY TRANSPORT

We require two separate analyses for determining the rate of vaporization as a function of the vapor pressure and the droplet temperature. A diffusion analysis that is valid when the pressure at the interface is less than one atmosphere and a gas dynamic model that is valid when the vapor pressure is equal to or greater than one atmosphere. In the diffusion analysis the kinetic energy of the vapor may be neglected and in the gas dynamic analysis heat conduction may be neglected. These two situations are shown in Fig.2.

Our primary interest is in propagation where the droplets are heated for times much longer than the diffusion time. Droplet evaporation can then be described by a quasi-steady analysis. In the notation of Ref. 17 the equations for mass and energy conservation are

$$\frac{d}{dr}\left(\left(\frac{r^2 cD}{1-X}\right)\frac{dX}{dr}\right) = 0 , \quad \dot{m}\sigma^2 C_p^v \frac{dT}{dr} = \frac{d}{dr}\left(\kappa r^2 \frac{dT}{dr}\right) , \tag{4}$$

subject to

$$X(r=\sigma) = X(T_p) , \; T(r=\sigma) = T_p , \; X(r=\infty) = X_\infty , \; T(r=\infty) = T_\infty , \tag{5}$$

where X, the mole fraction, is the ratio of the partial pressure of water vapor to the ambient pressure, c (gm-moles/cm^3) is the molar density of the mixture, D=0.23cm^2/s is the diffusion coefficient and C_p^v = 2 J/gm-^{o}K is the specific heat of water vapor. The solutions[17] to the governing equations, under the assumption that κ and cD are constant, give the heat and mass flux as

$$\kappa T_r = \dot{m} C_p^v (T_p - T_\infty)/(\exp(\dot{m} C_p^v \sigma/\kappa) - 1), \tag{6}$$

$$\dot{m} = (p_\infty D/R_v T_\infty \sigma) \ln[(1-X_\infty)/(1-X)] \tag{7}$$

Equating Eq. (7) to Eq. (1) determines X as an implicit function of the ratio of the saturated vapor pressure to the ambient pressure. After approximating F(v) in Eq. (1) by $(1-v(\pi/2R_v T_p)^{\frac{1}{2}})$, we obtain

$$X^s(T_p) = X + [D(2\pi T_p/R_v T_\infty^2)^{\frac{1}{2}}(1-0.5\epsilon)/\epsilon\sigma] \ln[(1-X_\infty)/(1-X)] \tag{8}$$

where the temperature dependence of $X^s(T_p)$ is given by the Clasius-Clapeyron relation. Numerical results are generated by regarding the mole fraction X as the independent variable. For a given value of X, less than unity, we determine the heat flux, the mass flux, and the temperature from Eqs. (6), (7), and (8). These results, when substituted into Eq. (3), determine the absorbed irradiance. Because of the quasi-steady assumption the droplet heat capacity term, T_t, is set to zero in Eq. (3). The amount of droplet superheat is determined by the difference $X^s(T_p)-X$ in Eq. (8) and increases as the mass flux increases or the droplet radius decreases. For droplets greater than 10 μm the difference is negligible and thermodynamic equilibrium applies. For droplets less than 1 μm the difference is large and the droplet will not reach surface equilibrium. As $\sigma \to 0$, for a fixed droplet temperature, the mass flux approaches a value independent of the radius whereas the heat conducted into the atmosphere increases like $1/\sigma$. Thus we will always reach a final droplet size where virtually all of the

absorbed energy heats the atmosphere. This is in contrast to the conclusion reached when surface equilibrium is assumed; namely, that most of the absorbed energy vaporizes the droplet. The importance of non-equilibrium effects has been emphasized in Refs. 1 and 5 and the above steady state diffusion analysis is due to Williams[1].

As the partial vapor pressure $X(T_p)$ approaches unity the diffusion model is no longer valid and must be replaced by the convective model shown in Fig. 2. Initially the vapor pressure exceeds the ambient pressure and drives a shock wave in to the atmosphere. The discontinuity occuring across the shock wave relates the pressure at the droplet surface to the vapor Mach number

$$M_v = 0.517(373/T_p)^{\frac{1}{2}}(p/p_\infty - 1)/[1+0.857(p/p_\infty - 1)]^{\frac{1}{2}}. \qquad (9)$$

As time increases the vapor bubble expands more slowly than the shock and remains seperated from the shocked air by a contact discontinuity. When $R_c > \sigma$ the influence of the shock is small. For a beam with irradiances of the order of a few kw/cm the vapor Mach number is subsonic and the flow field behaves as a quasi-steady, subsonic compressible point source. The pressure at the droplet surface is related to the vapor Mach number and ambient pressure p_∞ by

$$p = p_\infty/[1+(\gamma-1)M_v^2/2]^{\gamma/(\gamma-1)}, \qquad (10)$$

and is valid for $M_v < 1.0$ and $R_c > \sigma$. In Eq. (10), $\gamma = 1.3$ is the adiabatic exponent of water vapor. The pressure at the droplet surface relaxes from the initial value

given by Eq. (9) to a value slightly less than one atmosphere in a few acoustic times. For a 1 μm droplet this occurs in times less than 0.1 μs. For a subsonic point source the velocity decreases and the pressure increases as the distance from the droplet increases. The ambient or stagnation pressure p_∞ is attained when the radius expands to twelve times the initial droplet size. Once ambient pressure is reached in the vapor sphere further change occurs by diffusion and it is during the cooling down of the vapor sphere that the energy, the sum of the vapor enthalpy and the kinetic energy terms in Eq. (3), gets deposited into the atmosphere as heat. The droplet temperature and mass flux are determined as a function of Mach number from Eq. (1), after replacing $\dot{m}$ by pv/R_vT_p and using Eq. (10) for the pressure. The energy balance at the droplet surface, Eq. (3), then determines the absorbed irradiance as a function of the mass flux.

In Fig. 3 we present the change in droplet temperature as a function of the absorbed irradiance for three representative droplets and two values of the evaporation coefficient. The droplets were initially at 288°K. The results were generated from both the diffusion and the convective analysis. For droplets heated volumetrically $3Q_a/4\sigma$ reduces to the bulk absorption coefficient α_p. At 3.8 μm, α_p is approximately 100/cm and the irradiance varies from 10^2 w/cm to 10^6 w/cm in Fig. 3. At 10.6 μm, α_p is approximately 1000/cm and the irradiance varies from 10^1 w/cm to 10^5 w/cm. The solid lines are for a evaporation coefficient of 0.04 and the dashed lines for an evaporation coefficient of 1.0. The 10 micron droplet, with $\epsilon = 1.0$, is the only case that exhibits quasi-equilibrium behaviour over a wide range of absorbed irradiances.

An even more important quantity required in high-energy laser beam propagation is the fraction of absorbed energy,

$$f = [\kappa T_r + \dot{m}(C_p^v(T_p - T_\infty) + v^2/2)]/[\kappa T_r + \dot{m}(L + C_p(T_p - T_\infty) + v^2/2)], \qquad (11)$$

that heats the atmosphere. This is presented in Fig. 4 as a function of the absorbed irradiance. The various regimes of droplet vaporization are clearly illustrated for the 10μm droplet. For absorbed irradiances less than 10^4 W/cm^3 diffusive transport dominates. In this regime the heat conduction term κT_r is the primary contributor to f. As the irradiance is increased f decreases, at first, because of the exponential decay of κT_r on $\dot{m}$. The relatively flat minimum represents the transition between diffusion and convection. In this regime the vapor enthalpy term, $\dot{m} C_p^v(T_p - T_\infty)$, is the important term in the numerator of Eq. (11). To the right of the minimum convection dominates and f increases because the stagnation enthalpy, the sum of the enthalpy and kinetic energy terms in Eq. (11), is increasing. Droplets other than 10μm also exhibit the same general behaviour. For those droplets larger than 10μm the minimum is reached at lower absorbed irradiances and for those droplets smaller than 10μm the minimum is reached at higher irradiances. We also note in Fig. 4 the difference in results for the two evaporation coefficients. When the evaporation coefficient is 1.0 at least 50% of the absorbed energy is available for vaporizing the droplets. When the evaporation is 0.04 only the larger droplets are readily vaporized. For a laser propagating in the atmosphere the appropriate evaporation coefficient is 0.04 and these results indicate that water droplets have longer lifetimes than previously expected.

Mass conservation at the droplet surface,

$$\dot{\sigma} = -(1 - f(\sigma, I))Q_a I/4\rho_p L, \tag{12}$$

determines the change in radius. Eq. (12) must be integrated numerically because of the complicated dependence of f on σ and I. However the essential details of the numerical solutions can be determined from the behaviour of droplets volumetrically heated a few tens of degrees above the ambient temperature. For an evaporation coefficient of 0.04 and $3IQ_a/4\sigma \leq 10^4$ w/cm^3 we have

$$1-f = 1/(1.56 + 2.15/\sigma(\mu m)). \tag{13}$$

After setting $Q_a = 4\alpha_p\sigma/3$, substituting Eq. (13) into Eq. (12) and integrating we obtain the droplet radius in microns from

$$1.56 \ln(\sigma_o/\sigma) + 2.15(1/\sigma - 1/\sigma_o) = I\alpha_p t/3\rho_p L = \tau. \tag{14}$$

Results for initial droplets σ_o = 0.1, 1.0 and 10 microns are presented in Fig. 5 as a function of the normalized time $\tau = I\alpha_p t/3\rho_p L$. The solid lines are for an absorbed irradiance of 10^4 w/cm^3 and the dashed lines are for an absorbed irradiance of 10^6 w/cm^3. The actual physical time for the curves differ by a factor of a hundred. The results for $I\alpha_p = 10^4$ w/cm^3 were determined from Eq. (14) and numerical integration of Eq. (12) was used to determine the results at $I\alpha_p = 10^6$ w/cm^3. The only significant difference in the results for the two absorbed irradiances occurs for droplets greater than 1μm. Even after the time

has been normalized by the irradiance a 10 μm droplet initially vaporizes faster at the higher irradiances because more of the energy couples into vaporization. As the droplet vaporizes to submicron size the fraction of energy coupled into vaporization becomes equal for the two irradiances. In this regime, large τ in in Fig. 5, all droplets are approximately equal and independent of the initial size and absorbed irradiance. The final droplet size depends only on the normalized time and is given by Eq. (14).

IV. PROPAGATION ANALYSIS

We will now incorporate the single droplet results into an analysis for determining the irradiance distribution of a laser beam propagating in a hygroscopic aerosol. The equation describing the complex amplitutide A is the paraxial approximation to the scalar wave equation

$$2ikA_z + \nabla^2 A + 2k^2(\eta_\infty - 1)\rho A = -ik(\alpha_m + \alpha_e)A\,, \tag{15}$$

where $k = 2\pi/\lambda$ is the wave number, η_∞ is the refractive index of air, α_m is the molecular absorption coefficient, and α_e is the aerosol extinction coefficient. The density, ρ, induced by molecular and aerosol absorption can be determined from a simplified version of the hydrodynamics of heterogeneous media[18]. The variables that appear in the continuity, momentum and energy equations can be regarded as averaged over a gas volume containing many droplets. Use of the average values requires the regions of immediate influence of the droplets to dissipate rapidly over the gas volume. The vaporizing droplets act as distributed heat and mass sources. Multiplying the droplet energy balance, Eq. (3) by $4\pi\sigma^2 n(\sigma_o)$ and integrating over σ_o gives the total heat added to the atmosphere. Under the assumption that the heating occurs at constant pressure the steady state density perturbation induced by a moving aerosol is

$$\rho = -\left(\frac{(\gamma_\infty - 1)}{\gamma_\infty p_\infty}\right)\left(\int_0^t (\alpha_m + q_e(I))\, I(u, y, z, t')dt' \quad ; \; u = x - U(t-t')\right) \tag{16}$$

where γ_∞ is the ideal gas constant for air, p_∞ is the ambient pressure, U is

the velocity component transverse to the beam and q_e is the heat added to the atmosphere by the aerosol. The total extinction coefficient and the heat added to the atmosphere are defined by

$$\alpha_e = \int_0^\infty \pi\sigma^2(\sigma_o, I)Q_e(\sigma_o, I))n(\sigma_o)\, d\sigma_o \tag{17}$$

$$q_e = \int_0^\infty \pi\sigma^2(\sigma_o, I)f(\sigma, I)\, Q_a(\sigma(\sigma_o, I))n(\sigma_o)d\sigma_o \tag{18}$$

where $n(\sigma_o)$ is the initial droplet distribution function. The Mie absorption coefficient can be calculated using the following analytical approximation [19]

$$Q_a = 1-(1-(1+2\alpha_p\sigma)\exp(-2\alpha_p\sigma))/2(\alpha_p\sigma)^2;\ \alpha_p = 2k\eta_i \tag{19}$$

However the extinction coefficient should be calculated using the exact theory

$$Q_e = \sum_0^\infty (4n+2)Re(a_n + b_n)/\alpha_s^2\ ;\ \alpha_s = 2\pi\sigma/\lambda \tag{20}$$

Evaluation of the irradiance dependence of α_e and q_e requires solution of Eq. (12) for those droplets in the size range specified by $n(\sigma_o)$.

This completes the formulation for aerosol thermal blooming. The case of non-vaporizing particles such as carbon particles is obtained from the above analysis by setting $f(\sigma, I)=1$ and $\sigma = \sigma_o$ in Eqs. (17) and (18). The results for the extinction coefficient and the heat addition term q_e are sensitive to the laser wavelength and size distribution of the droplets.

Two droplet distribution functions that are much used for modelling aerosols are the modified gamma distribution of Deirmendjian and the power law distribution of Junge[19]

$$n(\sigma_o) = N(\sigma_o/\sigma_m)^a \exp(-b(\sigma_o/\sigma_m)^b) \; ; \quad n(\sigma_o) = N\sigma_o^{-a} \tag{21}$$

The parameters, in the modified gamma distribution for various types of aerosols, are

haze	a = 2	b = 4	c = .5	σ_m = .07 μm
rain	a = 2	b = 4	c = .5	σ_m = .07 μm
clouds	a = 8	b = 6	c = 1	σ_m = 4.0 μm

The parameters in the power law distribution for various types of aerosols are

haze	$3 < a < 4$	$.01 < \sigma_o < 10$
fogs-smokes	a=2	$.1 < \sigma_o < 20$
dust clouds	a=2	$.4 < \sigma_o < 4$

To complete the analysis we need only specify the real and imaginary parts of the index of refraction and typical mass extinction coefficients for battlefield aerosols. These aerosols include smokes that are hygroscopic, dust clouds, carbon smokes such as diesel exhaust and fog oil. At 10.6 μm these properties are summarized as follows:

	nr	ni	α_e (m^2/g)	α_a (m^2/g)
Red Phosphorus	1.8	0.389	0.244	0.218
fog Oil	1.48	0.163	0.168	0.167
Carbon Smokes	3.3	1.70	0.80	$>.9\alpha_e$
Dust Clouds			0.20	$>.5\alpha_e$

For non-vaporizing aerosols these results can be incorporated into the Army propagation codes by adding q_e, with f=1 and $\sigma = \sigma_o$, to the thermal blooming contribution and adding α_e with $\sigma = \sigma_o$, to the exponential term (i.e. $\exp(-(\alpha_m + \alpha_e)z)$). For vaporizing aerosols this is still correct except now we must compute f and σ with an aerosol subroutine that is called for each value of x, y, and time t. This subroutine then computes α_e and q_e using the local values of the irradiance $I(x, y, z)$, $\sigma(\sigma_o, t)$, and $f(\sigma, I)$. In order that this maybe accomplished the change in droplet size for each droplet in the droplet distribution function must be stored for each x and y. The Mie absorption and extinction using the new, vaporized, droplet sizes is then used to compute α_e and q_e. This value is then passed to the main propagation program.

For pulsed lasers this indicates that any relevant propagation calculation must be four dimensional. As an example of the magnitude of the calculation we must compute and store the change in droplet size for about 200 droplets at each value of x, y, and t , determine the 200 Mie extinction coefficients for these vaporized droplets, and do this for each transverse mesh point in the propagation calculation. For a transverse mesh point grid 64x64 and 20 z-steps about 10 million Mie extinction calculations are required in the typical propagation calculation. Since Mie scattering calculations are well known to be time consuming development of efficient algoritms are mandatory. The only other approach is to develop rational (analytical expressions) approximations to the Mie coefficients. Presently, accurate expressions over the entire droplet size range are not known. Until this is accomplised full numerical treatment of nonlinear aerosol thermal blooming is not possible.

REFERENCES

This work was supported by the U. S. Army Missile Research and Development Command under Contract DAAK40-76-C-1228.

1. F.A. Williams, "On vaporization of mist by radiation," Int. J. Heat and Mass Transfer 8, 575-587 (1965).

2. G. J. Mullaney, W. H. Christiansen and D. A. Russell, "Fog dissipation using a CO_2 laser," Appl. Phys. 13, 145 (1968).

3. G. W. Sutton, "Fog dispersal by high power lasers," AIAA J. 8, 1907(1970).

4. S. L. Glickler, "Propagation of a 10.6μm laser through a cloud including droplet vaporization," App. Opt. 10, 644 (1971).

5. G. E. Caledonia and J. D. Teare, "Aerosol propagation effects," J. Heat Transfer 99, 200 (1977). don't have journal

6. R. F. Lutomirski, W. L. Woodie, A.R. Hines and M. A. Dore, "Maritime aerosol effects on high energy laser propagation," Pacific Sierra Research Corp. PSR-510 (September 1975).

7. R.C. Harney, "Hole boring in clouds by high-intensity laser beams: theory," App. Opt. 16, 2974 (197).

8. S. M. Bedair and S. S. Aly, "Fog dissipation using 10.6μm radiation," Infrared Phys. 15, 233 (197).

9. P. Kalafas and A. P. Ferdinand, "Fog droplet vaporization and fragmentation by a 10.6μm laser pulse," Appl. Opt. 12, 29 (1973).

10. P. Kalafas and J. Hermann, "Dynamics and energetics of the explosive vaporization of fog droplets by a 10.6μm laser pulse," Appl. Opt. 12, 772 (1973).

11. J. E. Lowder, H. Kleimann and R. W. O'Neil, "High-energy CO_2 laser pulse transmission through fog," J. Appl. Phys. 45, 221 (1974).

12. M. C. Fowler, J. R. Dunphy and D. C. Smith, "Laser propagation experiments - aerosol and stagnation zone effects," United Technology Research Report R77-922578-13 (June 1977).

13. R. Cole, "Boiling nucleation," Progress in Heat and Mass Transfer, 8, 85(1975).

14. W. J. Bornhorst and G. N. Hatsopoulos, "Analysis of a liquid vapor phase change by the methods of irreversible thermodynamics," J. Appl. Mech. 34E, 840-846 (1967).

15. R. W. Schrage, A Theoretical Study of Interphase Mass Transfer (Columbia University Press, New York, 1953).

16. H. Merte, Jr., "Condensation heat transfer," Progress in Heat and Mass Transfer, 6, 181 (1973).

17. R. B. Bird, W. E. Stewart and E. N. Lightfoot, Transport Phenomena (Wiley, New York, 1960).

18. F.W. Marble, "Dynamics of dusty gases," Ann. Rev. Fluid Mech. 2, 399-447 (1970).

19. E. J. McCartney, Optics of the Atmosphere (Wiley, New York, 1976).

20. T. H. Cosden et al, "Atmospheric Transmission Measurement Report," Naval Research Laboratory Rep. 8104 (September 1977).

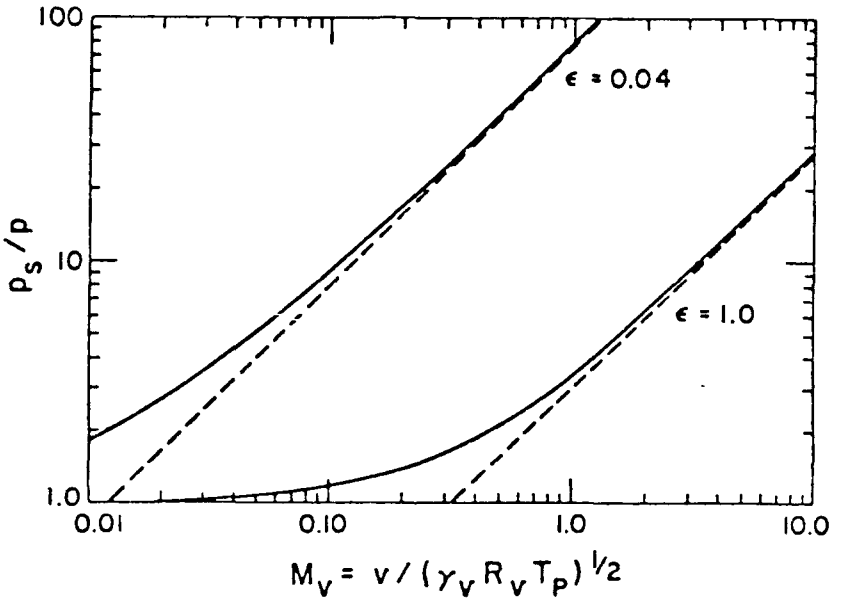

Fig.1 Mach number dependence of the ratio of the saturated vapor pressure to the actual vapor pressure. Amount of superheat is limited by the tensile strength of the droplet. Also shown are the asymptotes where collisions of the vapor molecules with the droplet are small.

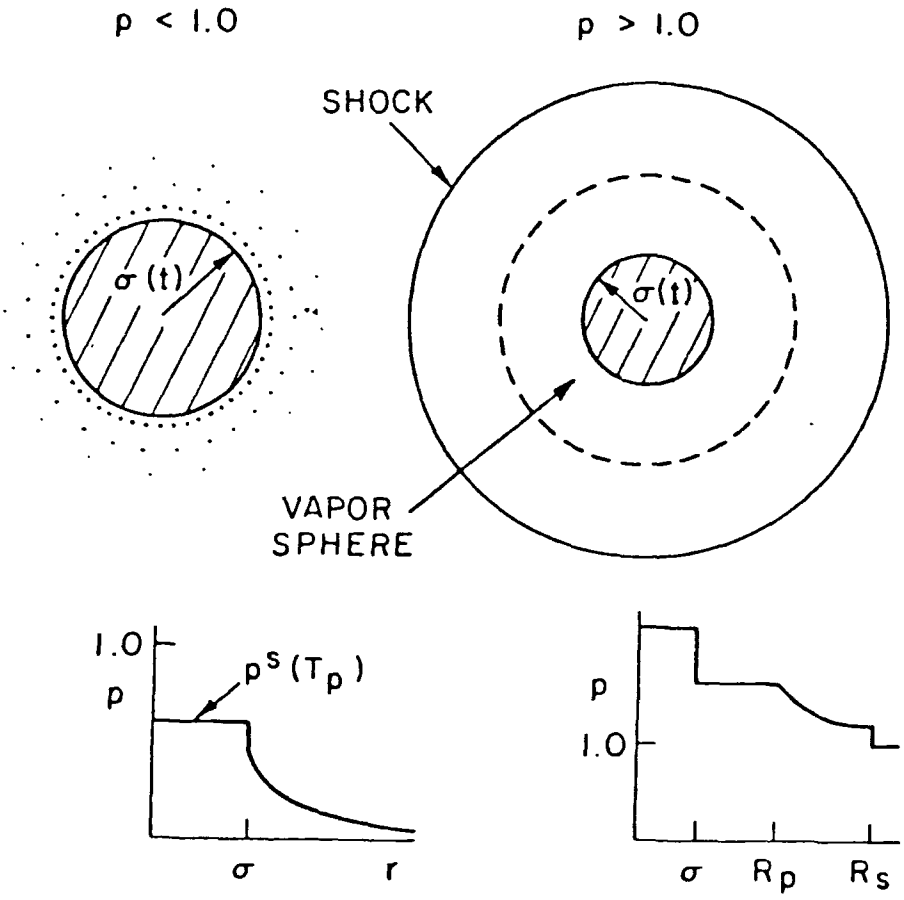

Fig. 2 Typical vapor pressure distributions for the diffusion and subsonic convective transport models. Interfacial discontinuities at the droplet surface are of the order of a mean free pathlength.

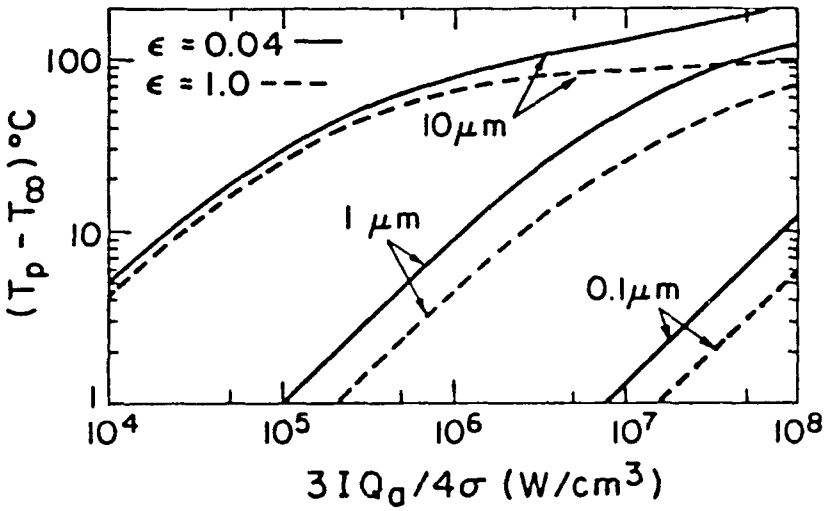

Fig. 3 Dependence of the peak droplet temperature on the absorbed irradiance. For droplets that absorb volumetrically the abscissa becomes $I\alpha_p$.

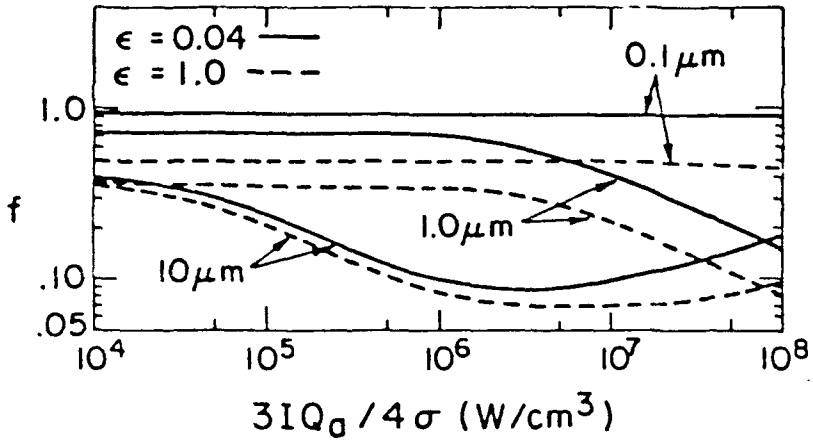

Fig. 4 Fraction of the absorbed energy that is deposited into the atmosphere as heat. The remainder of the absorbed energy vaporizes the droplet.

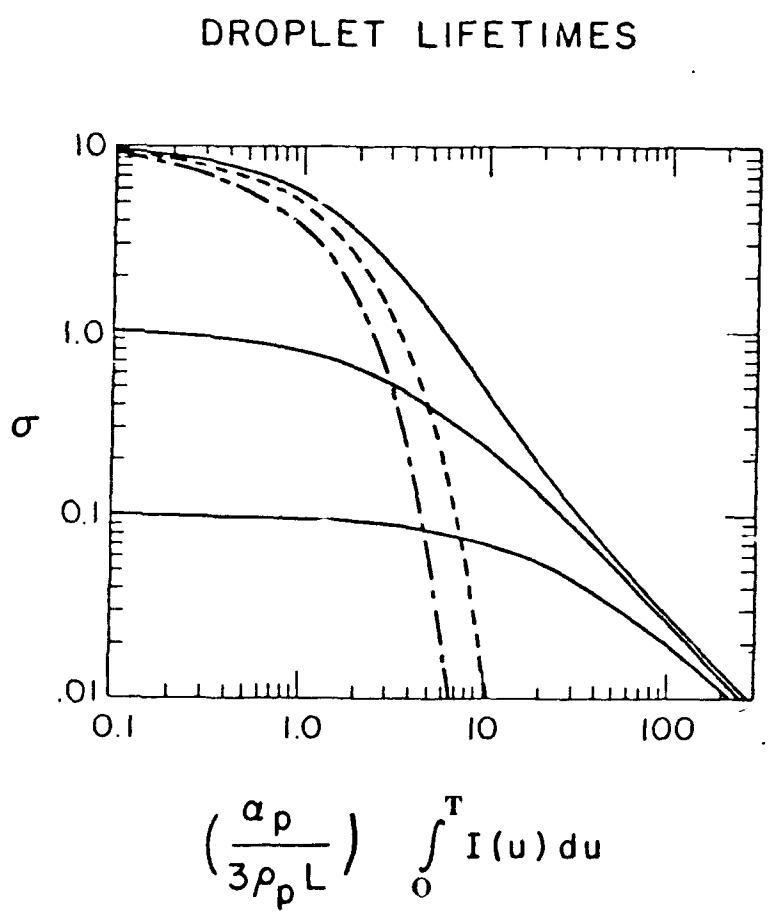

Fig. 5 Droplet lifetimes as a function of the absorbed irradiance. Also shown as the dashed lines are the lifetimes under the adiabatic and equilibrium assumptions.